ARTICLE

Tracking side reactions of the inverse vulcanization process and developing monomer selection guidelines

Received 00th January 20xx,
Accepted 00th January 20xx

DOI: 10.1039/x0xx00000x

Yusuke Onose,[a] Yuri Ito [a] Junpei Kuwabara *[a] and Takaki Kanbara *[a]

Recently, inverse vulcanization has attracted attention because of its utilization of surplus resources and the functionality of the resulting polymeric products. However, details of the byproducts and side reactions are not well known because most of the polymers obtained by inverse vulcanization have complex crosslinked structures, making it difficult to analyze the byproducts. The structures generated by side reactions may adversely affect physical properties; therefore, the objective of this study is to develop guidelines for monomer selection in inverse vulcanization. For this purpose, various olefin monomers were inverse-vulcanized, and their side reactions were traced. From the structural analysis of the products, we identified the terminal structures caused by chain transfer and the byproduct that may contribute to some of the coloration of the polymer. Subsequent evaluation of the thermal stability indicated that the terminal structures of the polymers obtained from aromatic and aliphatic terminal olefins increased upon heating. In contrast, the polymer obtained from aliphatic internal olefin is stable with no such structural changes. These results provide the guidelines for monomer selection in inverse vulcanization.

Introduction

The combustion of sulfur-containing fossil fuels produces sulfur oxides, which cause acid rain and environmental pollution.[1] Therefore, desulfurization of fossil fuels is an important refining process from an environmental protection perspective. However, excess sulfur is a global problem. Although sulfur is an essential raw material for the manufacturing of sulfuric acid and vulcanized rubber, annually produced 70 million tons of sulfur are far exceeding consumption. Recently, Pyun et al. developed an inverse vulcanization method to produce sulfur-rich polymers through the simple mixing of olefins and sulfur at high temperatures.[2–4] This method is expected to solve the problem of excess sulfur because it is effectively utilized in atom-economical processes.

Sulfur-rich polymers have been actively investigated for various applications,[5] such as cathode materials for Li–S batteries,[6–8] infrared permeable materials,[9–11] self-healing materials,[12,13] metal trapping materials[14,15] and adhesives.[16,17] The development of valuable functional materials can be achieved by using sulfur, which is an inexpensive raw material owing to its surplus resources.

Inverse vulcanization is based on the addition reaction of olefins with sulfur radicals generated by the homolysis of S–S bonds at high temperatures (Fig. 1). Various types of olefinic compounds have been used as co-monomers. Aromatic olefins are widely used as olefin monomers such as diisopropenyl benzene (DIB)[3,18,19] and divinyl benzene (DVB)[20–22] in the study of inverse vulcanization. Recently, not only aromatic olefins but also aliphatic olefins[9,23–27] have been used as comonomers of sulfur. The inverse vulcanization of sustainable biomass has also been reported, including limonene[9,24] and unsaturated fatty acids.[25–27] Previous studies mainly used monomers with multiple reaction points, which produced crosslinked structures. While crosslinked structures improve the mechanical properties of the product, detailed structural analysis is difficult because of their insolubility in solvents; therefore, their structures and byproducts are not well understood. If polymerization occurs only via radical addition to the olefin monomers, the polymers obtained from inverse vulcanization are simple poly-thioethers and polysulfide moieties. The absorption wavelengths of simple poly-thioethers should not be in the visible region and polymers with no absorption in the visible region have been synthesized using the inverse vulcanization method.[28] However, there have been some reports on polymers colored red, orange, yellow, or black.[3,20,22] Therefore, by-products are expected to contribute to the coloration of the polymer. Because undesired byproducts may adversely affect the properties of the polymer, it is important to know the side reactions that may occur and select monomers that can suppress them. A previous study revealed that chain transfer reactions form terminal and branched structures. [29]

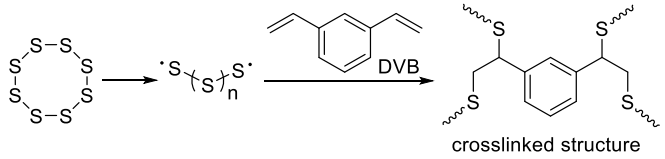

Figure 1. Main reaction of the inverse vulcanization.

[a] Tsukuba Research Center for Energy Materials Science (TREMS), Graduate School of Pure and Applied Sciences, University of Tsukuba, 1-1-1 Tennodai, Tsukuba, Ibaraki 305-8573, Japan. E-mail: kanbara@ims.tsukuba.ac.jp, kuwabara@ims.tsukuba.ac.jp

†Electronic Supplementary Information (ESI) available: See DOI: 10.1039/x0xx00000x

In this study, monomers with only one olefin moiety were selected to synthesize a soluble polymer with minimal crosslinking for a detailed analysis of their structure and side reactions (Fig. 2). We aim to establish guidelines for selecting suitable monomers from internal, terminal, or exo-olefins, which are less prone to side reactions, through the identification of byproducts and comparison of the structure and physical properties of the products.

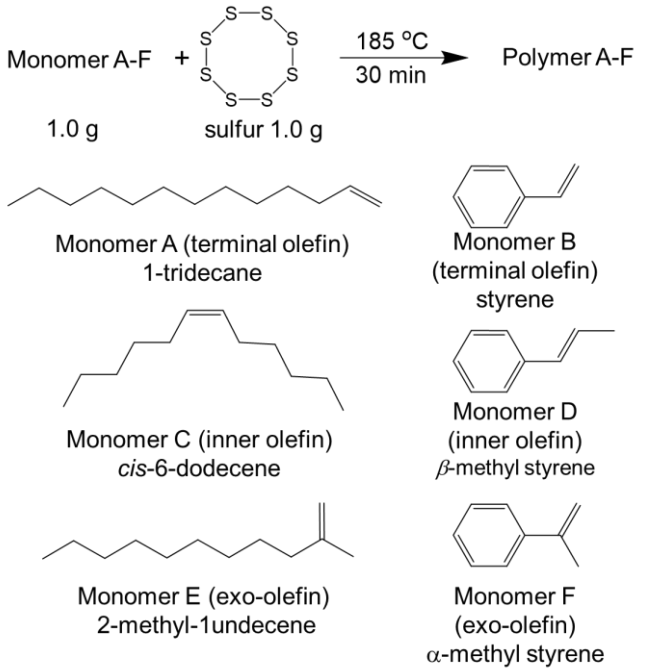

Figure 2. Structure of monomer A–F.

Results and discussion

Inverse vulcanization of monomers A–F was performed (Fig. 2). Aliphatic and aromatic, terminal olefins bearing, internal, and exo-olefins structures were selected as the monomers. The inverse vulcanization reactions of these monomers (S_8 : monomer = 1:1 in weight ratio) were conducted at 185 °C for 30 min.

Terminal olefin (Monomer A, B)

Inverse vulcanization of monomer A, an aliphatic terminal olefin compound produced Polymer A with a 76% yield. The structural analysis of Polymer A was performed using the NMR spectra shown in Fig. 3. Based on the ^{1}H NMR spectrum (Fig. 3a), consumption of the monomer was confirmed by the disappearance of the signal attributed to the olefinic moiety of the monomer. Based on the ^{13}C{^{1}H}, DEPT-135°, and DEPT-90° NMR spectra (Fig. 3b), two signals attributed to tertiary carbons were observed: carbon signal at 52 ppm (**d**) and carbon signal at 48 ppm (**g**). The presence of these two signals indicates that two types of structures were present in the product: the main and terminal structures. The main structure is a linear structure formed by radical addition. Four signals were observed from 3.1 to 3.7 ppm in the ^{1}H NMR spectrum (Fig. 3a). The H–H COSY spectrum (Fig. 3c) shows that the proton signal **g** at 3.1 ppm is coupled with the proton signal **h** at 1.4 ppm attributed to the

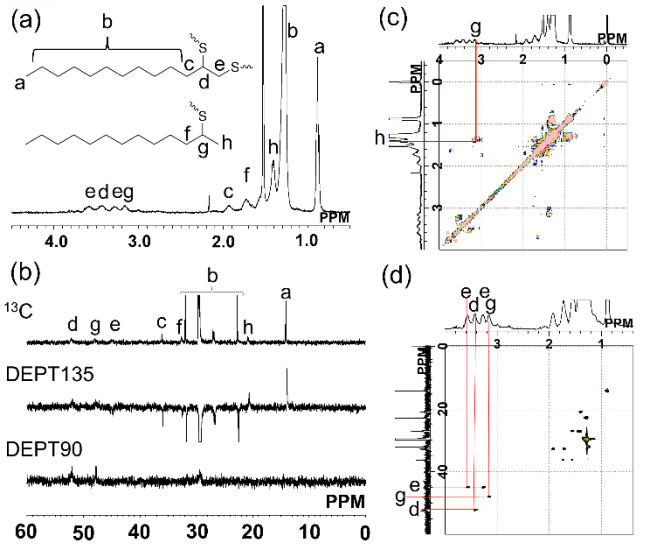

Figure 3. NMR spectra of Polymer A. (a)^{1}H NMR spectrum (600 MHz, $CDCl_3$, r.t.). (b)^{13}C{^{1}H} NMR spectra (100 MHz, $CDCl_3$, r.t.). (c)H-H COSY spectrum (400 MHz, $CDCl_3$, r.t.). (d)HSQC spectrum (400 MHz, $CDCl_3$, r.t.)

methyl proton. This terminal structure is caused by hydrogen abstraction of primary carbon radicals (Scheme 1).[29] Because the proton signal **d** is coupled with the tertiary carbon signal **d** at 52 ppm in the HSQC spectrum (Fig. 3d), the carbon signal **d** is attributed to the linear structure. The proton signals at 3.3 and 3.6 ppm are correlated with the ^{13}C{^{1}H} NMR carbon signal **e** at 44.7 ppm in the HSQC (Figs. 3b,3d). The signals **e** in the ^{1}H NMR spectrum (Fig. 3a) was split into two signals. This suggests that the neighboring carbon **d** has different chiral and torsional conformations in the center, resulting in a diastereotopic relationship with each other. Based on the integrated values of the ^{1}H NMR signals attributed to the terminal structure, the polymer was trimer on average.

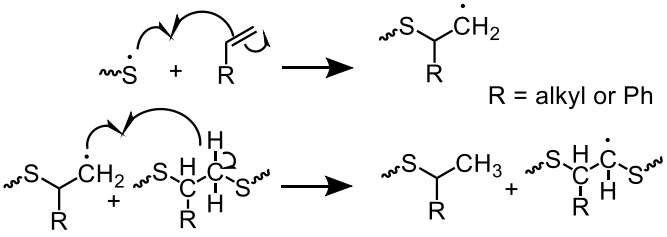

Scheme 1. Formation of terminal structure.[29]

Inverse vulcanization was performed using monomer B as an aromatic terminal olefin monomer. Consequently, the polymer was obtained with a 93% yield. In the ^{1}H NMR spectrum (Fig. 4a), the signal derived from the olefinic moiety of the monomer disappeared, confirming the consumption of the monomer.^{13}C{^{1}H}, DEPT-135°, and DEPT-90° NMR spectra (Fig. 4b) revealed two signals originating from tertiary carbons at 55 (**a**) and at 51 ppm (**c**), respectively. The proton **a** on the tertiary carbon atom correlates with the methylene proton signal **b** on

the H–H COSY (Fig. S1†). The proton on the tertiary carbon signal **c** is correlated with the methyl proton signal **d**. Thus, there are two structures: a linear structure and a methyl terminal structure as shown in Fig. 4a. Based on the integrated values of the ^{1}H NMR signals (Fig. 4a), Polymer B had a smaller percentage of terminal structures than Polymer A because monomer B underwent the reaction shown in Scheme 1 less frequently than monomer A. Polymer B was a trimer or a tetramer on average.

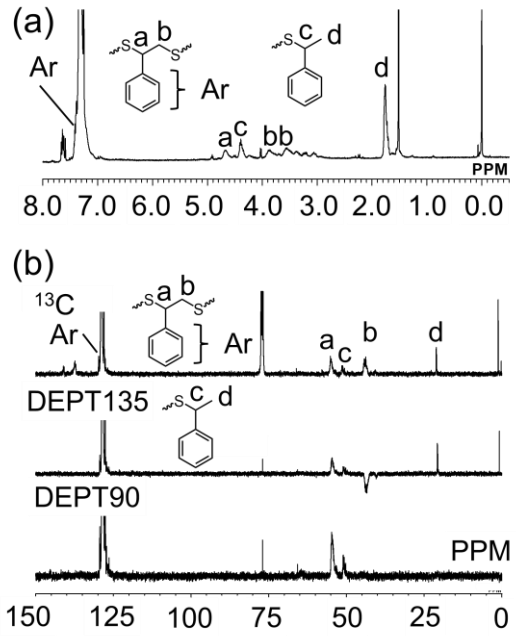

Figure 4. NMR spectra of Polymer B (a)^{1}H NMR spectrum (600 MHz, $CDCl_3$, r.t.), (b)^{13}C{^{1}H} NMR spectra (100 MHz, $CDCl_3$, r.t.).

Internal olefine (Monomer C, D)

Inverse vulcanization of monomer C resulted in 63% yield of Polymer C. The chemical structural analysis of Polymer C was conducted based on a study on the inverse vulcanization of long-chain internal olefin compounds. [30] The structure of the main product is shown in Fig. 5. The ^{1}H NMR spectrum (Fig. 5a) shows that the olefin signal disappeared, confirming the progress of the reaction. This result was further confirmed based on the ^{13}C{^{1}H} NMR, DEPT-90° DEPT-135° (Fig. 5b), H–H COSY (Fig. 5c), and HSQC spectra (Fig. 5d). ^{13}C{^{1}H} NMR, DEPT-90°, DEPT-135° spectra (Fig. 5b) showed that signal at 54 ppm (**f**) was a tertiary carbon in the main chain to which sulfur was directly attached. The carbon signal **a** at 14 ppm was identified as a methyl group at the end of the side chain, whereas signals **b**–**e** were identified as methylene group in the side chain. The signals in the ^{1}H NMR spectrum (Fig. 5a) were attributed to the methyl proton signal **a**, methine proton signal **f**, and methylene protons **b**–**e**. The H–H COSY (Fig. 5c) shows a correlation between signal **a** at 3.0 ppm and **e** at 1.6 ppm, indicating that signal **f** is a proton bonded to the carbon signal **f**, to which a sulfur is attached. HSQC (Fig. 5d) reveals that the proton signals **e** are correlated with the two carbon signals **e**. The presence of two carbon signals (**e**) are attributed to the diastereomeric form.

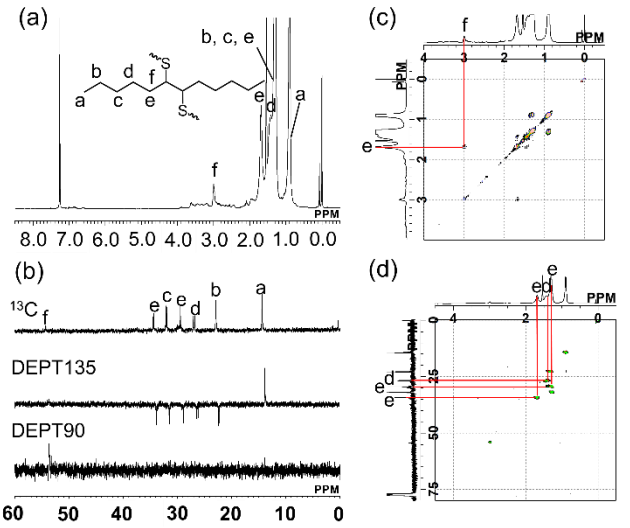

Figure 5. NMR spectra of Polymer C (a)^{1}H NMR spectrum (600 MHz, $CDCl_3$, r.t.), (b)^{13}C{^{1}H} NMR spectra (100 MHz, $CDCl_3$, r.t.), (c)H-H COSY spectrum (400 MHz, $CDCl_3$, r.t.), (d)HSQC spectrum (400 MHz, $CDCl_3$, r.t.).

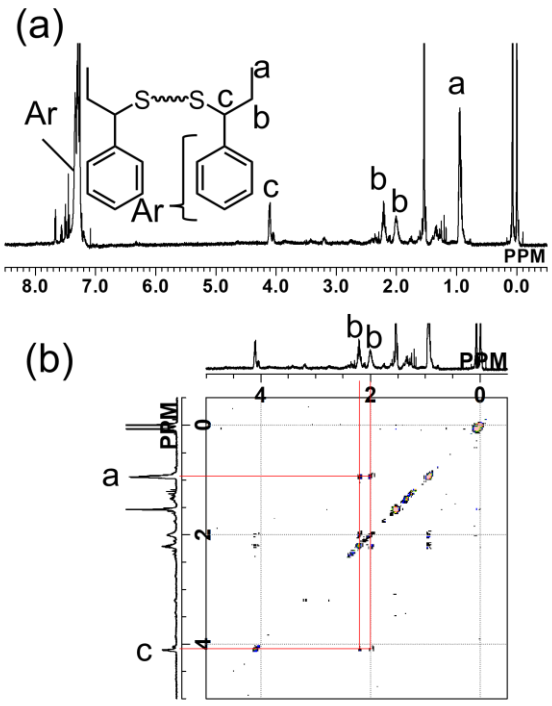

Figure 6. NMR spectra of dimer D (a)^{1}H NMR spectrum (600 MHz, $CDCl_3$, r.t.), (b)COSY NMR spectrum (400 MHz, $CDCl_3$, r.t.).

Inverse vulcanization was performed using monomer D as the aromatic internal olefin monomer. After the reaction, a yellow precipitate that was insoluble in the organic solvents was observed. The precipitate was identified as unreacted sulfur (32wt%) by DSC analysis. After filtration of the unreacted sulfur, the product was obtained with a 46% yield. The ^{1}H NMR spectrum (Fig. S3†) of the obtained compound confirms that

monomer D was not completely consumed. The complex spectrum suggested a mixture of various byproducts. For further analysis, the components were separated by column chromatography. The ^{1}H NMR spectrum of the separated component (37 mg, 9.3%) is shown in Fig. 6. The ^{1}H NMR spectrum (Fig. 6a) shows four main signals in the aliphatic region. The H–H COSY (Fig. 6b) reveals two proton signals **b** that correlate with both the methyl group proton signal **a** and the benzyl position proton signal **c**. These two **b** signals are non-equivalent methylene hydrogens owing to their location on carbon **b** next to chiral carbon **c**. The product has only the terminal structure. The product was reminiscent of the radical polymerization of β-alkyl styrene.[31,32] β-alkyl styrene has a significantly low reactivity owing to the large steric effect of the β-alkyl group in radical polymerization. In addition, the radical at the β position is stable owing to hyperconjugation; therefore, a sulfur radical was added to the benzyl position. The molecule with the radical generated by hydrogen withdrawal would have adopted a stable resonance structure, and thus no further reaction would have occurred (Scheme 2).[33] In contrast, Polymer C had a linear structure, as shown in Fig. 5. No further reduction in reactivity owing to hyperconjugation occurred because monomer C is not a conjugated monomer.

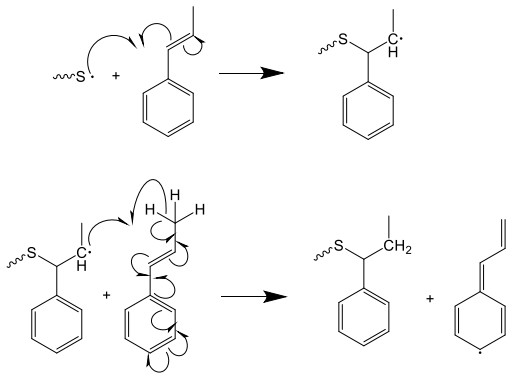

Scheme 2. Proposal chain transfer reactions. [33]

Exo-olefin (Monomer E, F)

Inverse vulcanization was performed with monomer E, an aliphatic exo-olefin monomer. The product was obtained with a 73% crude yield. ^{1}H NMR spectra (Fig. S4†) of the crude product confirmed the consumption of olefinic moieties. However, the signals appeared as multiple byproducts. The products were separated using silica gel column chromatography. The ^{1}H NMR spectrum of the separated compounds (Fig. 7a) showed a signal at 8.2 ppm, which could be attributed to the 1,2-dithiol-3-thione ring structure.[34] This structure is designated as Structure (1) and obtained with a 1% yield. In addition, another 1,2-dithiol-3-thione structure was also confirmed and designated as Structure (2).

Inverse vulcanization was performed using monomer F as an aromatic exo-olefin model compound. Similar to monomer D, unreacted 23wt% sulfur remained after the reaction. After filtration, the products were obtained with a 46% crude yield. The ^{1}H NMR spectrum of the crude product (Fig. S5†) revealed the presence of several byproducts. The products were separated using column chromatography. The ^{1}H NMR spectrum of the separated byproduct is shown in Fig. 7b. As with aliphatic olefin monomer E, a signal was observed in the low-field region at 8.4 ppm, which is attributed to the 1,2-dithiol-3-thione ring. This structure was designated as Structure (3).

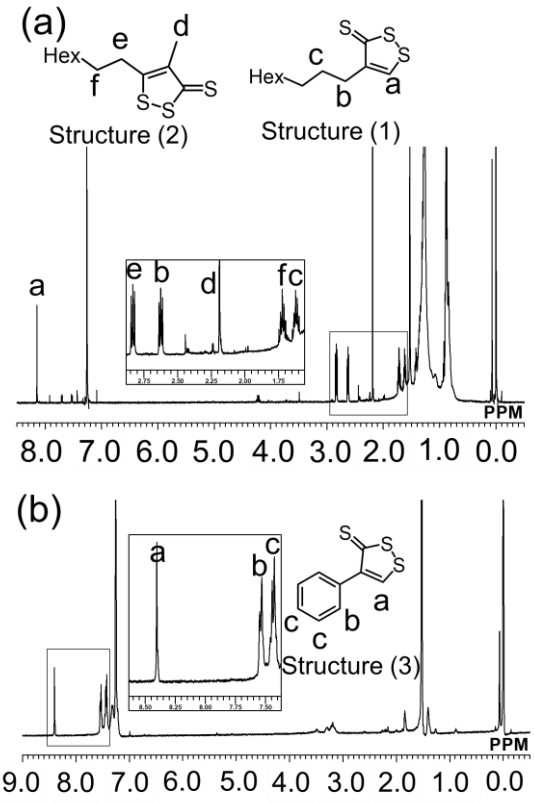

Figure 7. (a)^{1}H NMR spectrum of structure (1) and (2) (600 MHz, $CDCl_3$, r.t.), (b) ^{1}H NMR spectrum of structure (3) (600 MHz, $CDCl_3$, r.t.).

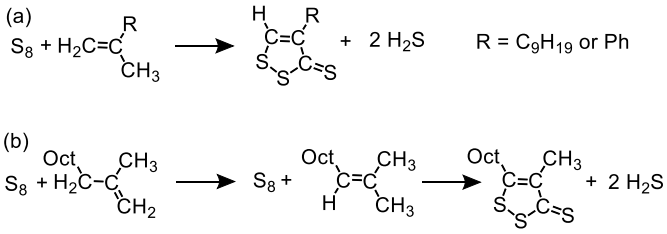

Scheme 3. Proposal byproduct formation process.[34]

It has been reported that 1,2-dithiol-3-thione derivatives can be obtained by heating exo-olefin compounds and diphosphorus pentasulfide at approximately 200 °C.[35] Hence, byproducts were generated in the process shown in Scheme 3a.[34] The internal transfer of the exo-olefin moiety (Scheme 3b) could produce isomer Structure (2). [34] Furthermore, the formation of 1,2-dithiol-3-thione byproducts was confirmed by absorption and IR spectroscopy and GC-MS (Fig. S6†). The UV-vis absorption spectra of the byproduct (Figs. 8a,8b) exhibit an absorption peak at a wavelength of 250 nm, originating from

the n → σ* transition of the S–S bond; absorption in the visible region was observed at a wavelength of 430 nm, originating from the 1,2-dithiol-3-thione rings,[36] for the aliphatic and aromatic groups. The absorption at 430 nm was caused by the orange color of the sample after the reaction. The orange-colored polymer[2] synthesized via inverse vulcanization is also thought to contain cyclic compounds as byproducts. The FT-IR spectra of these compounds revealed a peak attributed to the C=S bond at approximately 1200 cm^{-1} (Figs. 8c,8d).

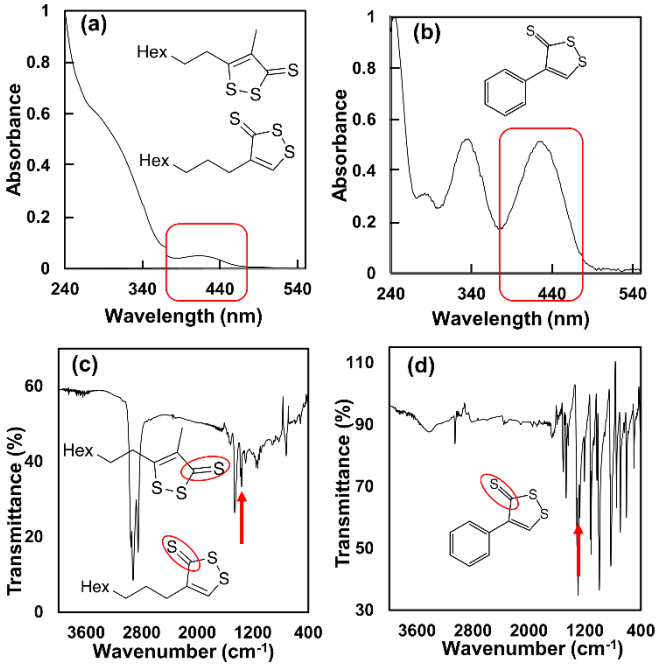

Figure 8. UV-vis absorption spectra in hexane and FT-IR spectra of the byproducts.

Stability Comparison

The stabilities of the polymers obtained from monomers A, B, and C was compared.[29] Each polymer was heated to 130 °C for a specified period. Heat-induced structural changes were observed using ^{1}H NMR spectroscopy (Fig. 9). Focusing on the terminal methyl group of Polymer A (from aliphatic terminal olefins), we observed that the integral value gradually increased with heating time. Using proton signal **d** in Fig. 9a, attributed to the methine proton of the linear structure, as 1.00, the integrated value of signal **g**, which is attributed to the terminal structure, increased from 1.02 to 1.36. Because the primary carbon radical is generated by the cleavage of the C–S bond and the radical draws hydrogen from the other polymer chains, a terminal methyl group is formed, as shown in Scheme 4. [29] The radicals generated by hydrogen abstraction are thought to recombine with sulfur radicals to form a branched structure. The integral value of hydrogen **e** decreased owing to the hydrogen abstraction by the primary carbon radicals. In Fig. 9b, the integrated value of signal **d** of the Polymer B increased from 0.75 to 0.89 with time. This indicates an increase in the terminal structure in the Polymer B as in the case of Polymer A.

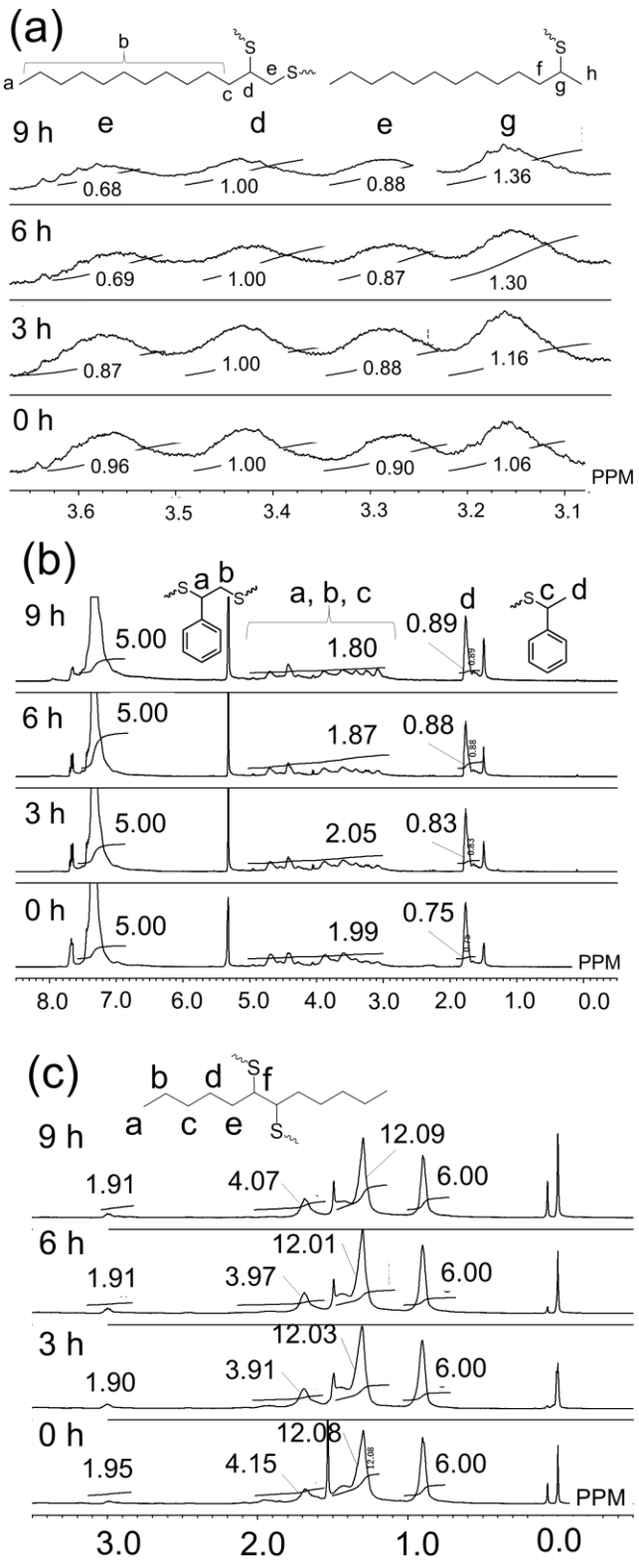

Figure 9. Comparison of ^{1}H NMR spectra for different heating times (a)Polymer A (400 MHz, $CDCl_3$, r.t.), (b)Polymer B (400 MHz, CD_2Cl_2, r.t.), (c)Polymer C (400 MHz, $CDCl_3$, r.t.).

In contrast, the ^{1}H NMR spectra of Polymer C (Fig. 9c) showed that the heat-inducted structural changes were only slightly observed for Polymer C. These results indicate that the most stable polymer for heating is Polymer C, which is obtained from aliphatic internal olefins.

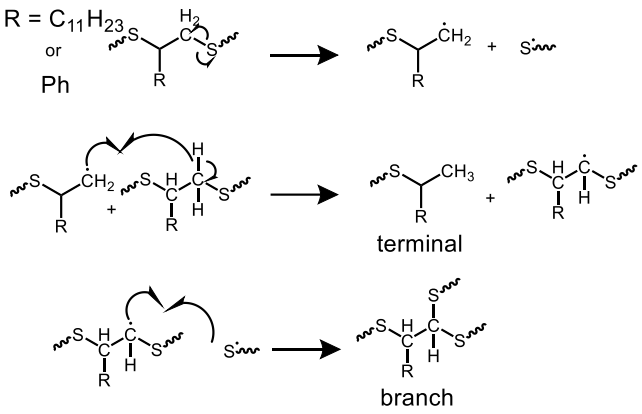

Scheme 4. Proposal structural changes by heating. [29]

Measurement of hydrogen sulfide generation

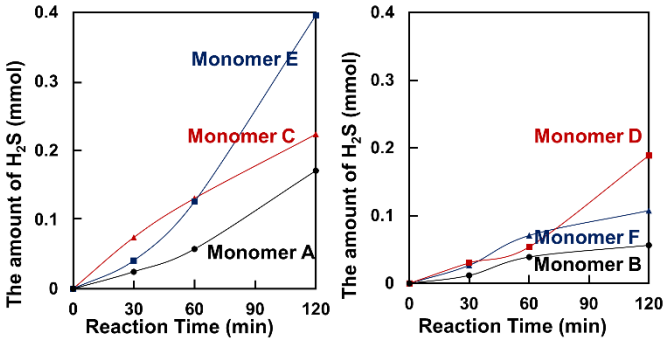

Figure 10. Comparison of hydrogen sulfide generation in inverse vulcanization.
(Left: Aliphatic monomer, Right: Aromatic monomer)

It has been reported that hydrogen sulfide is produced by side reactions of inverse vulcanization.[37] Therefore, the amount of hydrogen sulfide produced was also measured. As shown in Fig. 10, hydrogen sulfide was still generated after olefins were consumed. To suppress the generation of hydrogen sulfide owing to side reactions, it is necessary to set appropriate reaction times. Among the three aliphatic olefins, exo-olefins produced the highest amount of hydrogen sulfide. This could be because of the generation of hydrogen sulfide via the formation of a 1,2-dithiol-3-thione ring (Scheme 3). Monomers D and F produced more hydrogen sulfide than monomer B. This is because of the formation of terminal (Scheme 2) and cyclic (Scheme 3) structures via side reactions. Compared to aliphatic olefins, aromatic olefins produced less hydrogen sulfide. This is because the hydrogen is unlikely to be withdrawn from the benzene ring.[38]

Conclusions

This study revealed that aliphatic internal olefins are suitable monomers for suppressing side reactions. The structure of the by-product, such as the 1,2-dithiol-3-thione ring generated by inverse vulcanization, was identified by NMR spectra analysis. Furthermore, the presence of a 1,2-dithiol-3-thione ring was confirmed by UV-vis absorption. A stability test revealed that the most stable product was Polymer C, which was obtained from an aliphatic internal olefin. Polymer C is stable because its structure does not allow the formation of terminal methyl groups owing to hydrogen withdrawal. Hence, guidelines for monomer selection suitable for suppressing side reactions were obtained.

Experimental

Materials

Elemental sulfur and chroloform-d1 were purchased from Kanto Chemical Co., Inc. 2-Methyl-1-undecene and sodium amide were purchased from Sigma-Aldrich Co., Inc. Myristic acid, palladium chloride, bis[2-[(oxo)diphenylphosphino]phenyl] ether (DPE-Phos), 1,3-dimethyl-3,4,5,6-tetrahydro-2(1H)-pyrimidinone (DMPU), pivalic anhydride, triethyl amine, hexanal, hexyltriphenylphosphonium bromide, and potassium t-butoxide were purchased from Kanto Chemical Co., Inc. and used without further purification. Styrene, α-methyl styrene, and β-methyl styrene were purchased from Kanto Chemical Co., Inc. and distillated before use. Monomers A[39] and C[40] were synthesized according to the paper.

Measurements

^{1}H and ^{13}C {^{1}H} NMR spectra were recorded on a Bruker AVANCE 400 and AVANCE 600 NMR spectrometers at room temperature with TMS (0.00 ppm for ^{1}H NMR), $CDCl_3$ (77.0 ppm for ^{13}C NMR) as internal references. Differential scanning calorimetry (DSC) was conducted in aluminium pans using SHIMADZU Scientific Instrument Inc. DSC-60 Plus. The condition of DSC was under 50.0 ml min^{-1} N_2 flow, with heating and cooling rates of 5 °C min^{-1}. UV-vis absorption spectra were recorded in hexane on Jasco V-630 UV-Vis Spectrophotometer. Fourier transform infrared (FT-IR) spectra were recorded on JASCO FT-IR 4600 spectrometer. GC-MS spectra were recorded on SHIMADZU Scientific Instrument Inc.GC-MS-QP2010.

General procedure of polymerization (aliphatic model monomer A, C, E)

Elemental sulfur and each model monomer were placed in a 10 mL open grass vial. Then the mixture was stirred (550 rpm) at 185 °C for 30 minutes by using aluminium heating blocks. The total mass of the elemental sulfur and each model monomer were fixed at 2.00 g.

Inverse vulcanization of model monomer A. The product was obtained in 76% yield.

Inverse vulcanization of model monomer C. The product was obtained in 63% yield.

Inverse vulcanization of model monomer E. The product was separated by silica gel column chromatography using hexane and EtOAc(9:1) as an eluent. Structure (1) and (2) ware obtained in 1% yield. GC-MS Calcd. For $C_{12}H_{20}S_3$ 260.1, Found 259.6.

General procedure of polymerization (aromatic model monomer B, C, F)

Elemental sulfur and each model monomers were placed in a 25 mL Schlenk tube. A plastic tube was connected to the reactor and the end of the tube was dipped in a glass vial containing distilled water. Then the mixture was stirred (550 rpm) under nitrogen atmosphere at 185 °C for 30 minutes by using aluminium heating blocks. The total mass of the elemental sulfur and each model monomers were fixed at 2.00 g.

Inverse vulcanization of model monomer B. The product was obtained in 93% yield.

Inverse vulcanization of model monomer D. The product was separated by silica gel column chromatography using hexane and EtOAc (9:1) as an eluent. Dimer was obtained in 9% yield.

Inverse vulcanization of model monomer F. The product was separated by silica gel column chromatography using hexane and EtOAc (9:1) as an eluent. Structure (3) was obtained in 5% yield. GC-MS Calcd. For $C_9H_6S_3$ 210.0, Found 210.7.

The stability comparison of the polymer A, B, C [29]

The polymer A to C were heated to 130 °C for 9 hours under air. The ^{1}H NMR spectra are measured at regular intervals, respectively.

Identification of H_2S gas release[37]

The setup was similar to that of polymerization of the aromatic monomer with sulfur the vial glass connected to the reactor was filled with 1 M solution of silver nitrate ($AgNO_3$). As the reaction proceeded, the silver nitrate solution turned transparent to dark grey, and a dense black powder settled to the bottom of the vial. The formed black precipitation (Ag_2S) was filtered and weighted to analyse the amount of released H_2S gas.

Conflicts of interest

There are no conflicts to declare.

Acknowledgements

The authors thank the Chemical Analysis Division and the OPEN FACILITY, Research Facility Center for Science and Technology, University of Tsukuba, for the measurements of NMR. This research was partly supported by the Sasakawa Scientific Research Grant from the Japan Science Society (no. 2021-3013) and Toshiaki Ogasawara Memorial Foundation. One of the authors (Y. O.) is grateful to Japan science and Technology Agency (JST) for funding through Support for Pioneering Research Initiated by the Next Generation.

Notes and references

1 A. Riaz, M. Saeed, M. Munir, A. Intisar, S. Haider, S. Tariq, N. Hussain, R. Kousar and M. Bilal, *Environ. Res.*, 2022, **212**, 113160.

2 W. J. Chung, J. J. Griebel, E. T. Kim, H. Yoon, A. G. Simmonds, H. J. Ji, P. T. Dirlam, R. S. Glass, J. J. Wie, N. A. Nguyen, B. W. Guralnick, J. Park, Á. Somogyi, P. Theato, M. E. Mackay, Y. E. Sung, K. Char and J. Pyun, *Nat. Chem.*, 2013, **5**, 518–524.

3 J. J. Griebel, S. Namnabat, E. T. Kim, R. Himmelhuber, D. H. Moronta, W. J. Chung, A. G. Simmonds, K. J. Kim, J. van der Laan, N. A. Nguyen, E. L. Dereniak, M. E. MacKay, K. Char, R. S. Glass, R. A. Norwood and J. Pyun, *Adv. Mater.*, 2014, **26**, 3014–3018.

4 T. S. Kleine, R. S. Glass, D. L. Lichtenberger, M. E. Mackay, K. Char, R. A. Norwood and J. Pyun, *ACS Macro Lett.*, 2020, **9**, 245–259.

5 T. Lee, P. T. Dirlam, J. T. Njardarson, R. S. Glass, and J. Pyun, *J. Am. Chem. Soc.*, 2022, **144**, 5–22.

6 S. Oishi, K. Oi, J. Kuwabara, R. Omoda, Y. Aihara, T. Fukuda, T. Takahashi, J. C. Choi, M. Watanabe and T. Kanbara, *ACS Appl. Polym. Mater.*, 2019, **1**, 1195–1202.

7 P. T. Dirlam, R. S. Glass, K. Char and J. Pyun, *J. Polym. Sci. A Polym. Chem.*, 2017, **55**, 1635–1668.

8 P. Dong, K. S. Han, J. I. Lee, X. Zhang, Y. Cha and M. K. Song, *ACS Appl. Mater. Interfaces*, 2018, **10**, 29565–29573.

9 J. Kuwabara, K. Oi, M. M. Watanabe, T. Fukuda and T. Kanbara, *ACS Appl. Polym. Mater.*, 2020, **2**, 5173–5178.

10 T. S. Kleine, T. Lee, K. J. Carothers, M. O. Hamilton, L. E. Anderson, L. Ruiz Diaz, N. P. Lyons, K. R. Coasey, W. O. Parker, L. Borghi, M. E. Mackay, K. Char, R. S. Glass, D. L. Lichtenberger, R. A. Norwood and J. Pyun, *Angew. Chem. int. ed.*, 2019, **131**, 17820–17824.

11 L. Fang, J. Sun, X. Chen, Y. Tao, J. Zhou, C. Wang and Q. Fang, *Macromolecules*, 2020, **53**, 125–131.

12 J. J. Griebel, N. A. Nguyen, S. Namnabat, L. E. Anderson, R. S. Glass, R. A. Norwood, M. E. Mackay, K. Char and J. Pyun, *ACS Macro Lett.*, 2015, **4**, 862–866.

13 Y. Xin, H. Peng, J. Xu and J. Zhang, *Adv. Funct. Mater.*, 2019, **29**, 1808989.

14 M. P. Crockett, A. M. Evans, M. J. H. Worthington, I. S. Albuquerque, A. D. Slattery, C. T. Gibson, J. A. Campbell, D. A. Lewis, G. J. L. Bernardes and J. M. Chalker, *Angew. Chem. int. ed.*, 2016, **128**, 1746–1750.

15 D. J. Parker, H. A. Jones, S. Petcher, L. Cervini, J. M. Griffin, R. Akhtar and T. Hasell, *J. Mater. Chem.*, 2017, **5**, 11682–11692.

16 S. J. Tonkin, C. T. Gibson, J. A. Campbell, D. A. Lewis, A. Karton, T. Hasell and J. M. Chalker, *Chem. Sci.*, 2020, **11**, 5537–5546.

17 C. Herrera, K. J. Ysinga and C. L. Jenkins, *ACS Appl. Mater. Interfaces*, 2019, **11**, 35312–35318.

18 S. Zhuo, Y. Huang, C. Liu, H. Wang and B. Zhang, *Chem. Commun.*, 2014, **50**, 11208–11210.

19 A. G. Simmonds, J. J. Griebel, J. Park, K. R. Kim, W. J. Chung, V. P. Oleshko, J. Kim, E. T. Kim, R. S. Glass, C. L. Soles, Y. E. Sung, K. Char and J. Pyun, *ACS Macro Lett.*, 2014, **3**, 229–232.

20 C. R. Westerman and C. L. Jenkins, *Macromolecules*, 2018, **51**, 7233–7238.

21 K. Orme, A. H. Fistrovich and C. L. Jenkins, *Macromolecules*, 2020, **53**, 9353–9361.

22 L. J. Dodd, Ö. Omar, X. Wu and T. Hasell, *ACS Catal.*, 2021, **11**, 4441–4455.

23 K. S. Kang, A. Phan, C. Olikagu, T. Lee, D. A. Loy, M. Kwon, H. jong Paik, S. J. Hong, J. Bang, W. O. Parker, M. Sciarra, A. R. de Angelis and J. Pyun, *Angew. Chem. Int. Ed.*, 2021, **60**, 22900–22907.

24 L. Sun, S. Gao, X. Gui, L. Liu, K. Xu and H. Liu, *Eur. Polym. J.*, 2020, **123**, 109440.

25 A. D. Smith, C. D. McMillen, R. C. Smith and A. G. Tennyson, *J. Polym. Sci.*, 2020, **58**, 438–445.

26 C. Ni, D. Chen, Y. Zhang, T. Xie and Q. Zhao, *Chem. Mater.*, 2021, **33**, 2046–2053.

27 Y. Chen, A. Yasin, Y. Zhang, X. Zan, Y. Liu and L. Zhang, *Materials,* 2020, **13**, 632.

28 W. Jang, K. Choi, J. S. Choi, D. H. Kim, K. Char, J. Lim and S. G. Im, *ACS Appl. Mater. Interfaces*, 2021, **13**, 61629–61637.

29 Y. Zhang, J. J. Griebel, P. T. Dirlam, N. A. Nguyen, R. S. Glass, M. E. Mackay, K. Char and J. Pyun, *J. Polym. Sci. A Polym. Chem.*, 2017, **55**, 107–116.
30 P. Yan, W. Zhao, S. J. Tonkin, J. M. Chalker, T. L. Schiller and T. Hasell, *Chem. Mater.*, 2022, **34**, 1167–1178.
31 Y. Inaki, S. Hirose, S.-I. Nozakura and S. Murahashi, *Polym. J.,* 1972, **3**, 159-165.
32 A. Otsu, T. Ito and I. Irioto, *J. Polym. Sci. A Polym. Chem.*, 1964, **2**, 2901-2906.
33 L. Zhang, R. Liu, S. Lin and J. Xu, *Chem. Commun.,* 2021, **57**, 10759–10762.
34 P. S. Landis, *J. Chem. Eng. Data*, 1966, **11**, 412–413.
35 P. S. Landis, *Chem. Rev.*, 1965, **65**, 237–245.
36 R. Holland, M. Navamal, M. Velayutham, J. L. Zweier, T. W. Kensler and J. C. Fishbein, *Chem. Res. Toxicol.*, 2009, **22**, 1427–1434.
37 V. K. Shankarayya Wadi, K. K. Jena, S. Z. Khawaja, K. Yannakopoulou, M. Fardis, G. Mitrikas, M. Karagianni, G. Papavassiliou and S. M. Alhassan, *ACS Omega*, 2018, **3**, 3330–3339.
38 G. E. Davico, V. M. Bierbaum, C. H. DePuy, G. B. Ellison, and R. R. Squires, *J. Am. Chem. Soc.,* 1995, **117**, 2590-2599.
39 L. J. Gooßen and N. Rodríguez, *Chem. Commun.*, 2004, **4**, 724–725.
40 V. Difluoroalkanes and M. Schlosser, *Tetrahedron*, 1988, **44**, 2875-2881.

